**A TABLETOP APPARATUS TO MEASURE THE MAGNETIC MOMENT OF THE MUON**

By

David Richard Ely

A thesis submitted in partial fulfillment of the requirements for the degree of

Bachelor of Science

Houghton College

May 2002

Signature of Author………………………………………………………………...
Department of Physics
May 8, 2002

…………………………………………………………………………….
Dr. Mark Yuly
Associate Professor of Physics
Research Supervisor

…………………………………………………………………………….
Dr. Ronald Rohe
Associate Professor of Physics

# A TABLETOP APPARATUS TO MEASURE THE MAGNETIC MOMENT OF THE MUON

By

David Richard Ely

Submitted to the Department of Physics
on 8 May 2002 in partial fulfillment of the
requirement of the degree of
Bachelor of Science

**Abstract**

An apparatus was constructed to measure the magnetic moment of cosmic ray muons using their precession in a uniform magnetic field. A 102.0 × 20.6 × 5.4 cm plastic scintillator was sandwiched between two 102.0 × 20.6 × 1.6 cm scintillators inside a uniform, 42 G magnetic field, which was produced by a large solenoid. A small veto scintillator eliminated events occurring in the non-uniform region of the field at the ends of the solenoid. A logic circuit identified muons stopping in the center scintillator and the subsequent decay of these muons. The time difference between the muon stopping and its decay was recorded for about 67,000 events, allowing the decay constant and the magnetic moment to be determined.

Thesis Supervisor: Dr. Mark Yuly
Title: Associate Professor of Physics

TABLE OF CONTENTS


Chapter 1 INTRODUCTION ..... 1
1.1 History and Motivation ..... 1
1.2 Purpose ..... 2
1.3 Changes to the Previous Experimental Design ..... 3
1.3.1 Solenoid ..... 3
1.3.2 Detector Arrangement ..... 3
1.3.3 Triggers ..... 4
1.3.4 Timing Calibration Technique ..... 4
Chapter 2 THEORY ..... 6
2.1 Muon Characteristics ..... 6
2.2 Experimental Apparatus ..... 7
2.3 Muon Precession ..... 8
2.4 Muon Polarization ..... 9
2.5 Data Analysis ..... 11
Chapter 3 APPARATUS ..... 12
3.1 Tabletop Apparatus ..... 12
3.2 Solenoid ..... 13
3.3 Apparatus Components ..... 13
3.3.1 Scintillators ..... 14
3.3.2 Discriminators ..... 15
3.3.3 Logic Units ..... 15
3.3.4 Time to Amplitude Converter and Multichannel Analyzer ..... 17
3.4 Timing Calibration ..... 17
Chapter 4 RESULTS AND CONCLUSION ..... 19
Appendix A SOLENOID DESIGN ..... 21
Appendix B SCINTILLATOR AND PHOTOMULTIPLIER TUBE OPERATION ..... 23
Appendix C BACKGROUND DATA ..... 25
Appendix D MAGNETIC FIELD PRECESSIONAL DATA ..... 29

# LIST OF FIGURES

*Number* *Page*

Figure 1.1 .......... 4

Figure 2.1 .......... 7

Figure 2.2 .......... 9

Figure 2.3 .......... 10

Figure 3.1 .......... 12

Figure 3.2 .......... 13

Figure 3.3 .......... 16

Figure 3.4 .......... 18

Figure 4.1 .......... 20

Figure 4.2 .......... 20

Figure B.1 .......... 23

## ACKNOWLEDGMENTS

The author wishes to acknowledge my advisor, Dr. Yuly, for all of his patient instruction and help with this project. He worked very closely with my laboratory partner, Daniel Kroening, and me and was an integral part of our success. I would also like to acknowledge Daniel Kroening for his participation with me in this project. He was an excellent teammate with whom tasks could be shared and this project accomplished. My parents, Rick and Laura-Jo Ely, have encouraged me in my studies and been a great support. I want to thank them for supporting me and encouraging me to hang in there. My wife, Elizabeth Ely, has also been a wonderful encouragement. She has helped me by keeping me on task and even doing some of my chores.

*Chapter 1*

# INTRODUCTION

## 1.1 History and Motivation

Cosmic ray muons were first discovered by C. D. Anderson and S. H. Neddermeyer around 1936 in cosmic radiation [1]. Originally, they were thought to be electrons and positrons or protons. However, there were too many high energy electrons present in the radiation caused by the particles for them to be protons. On the other hand, the particles did not lose enough energy via bremsstrahlung as they traversed the atmosphere for them to be electrons or positrons. By placing a platinum plate in a cloud chamber, Anderson and Neddermeyer determined which particles of a given energy were strongly absorbed and which were highly penetrating. The results, however, did not fit any of the already known particles. Thus, it became "necessary to postulate the existence of positive and negative singly charged particles with a mass intermediate between the masses of the proton and the electron" [2]. These newly discovered particles were called mesotrons or mu mesons [3,2].

In 1935, Yukawa predicted the existence of mesons (intermediate mass particles) responsible for mediating the strong force [3]. Conversi, Pancini, and Piccioni showed in 1947, however, that mu mesons do not interact strongly enough with nucleons to be the particles predicted by Yukawa [4]. Just after this, Lattes, Muirhead, Occhialini, and Powell discovered pions [5,6], and it was shown that mu mesons were secondary particles formed in pion decay in the upper atmosphere [2]. They were more properly named muons at this point [3,2]. As it turned out, pions were the mesons Yukawa had predicted earning him the Nobel Prize in 1949 [7].

The spin precession of muons in a magnetic field has been studied in the past as a test of quantum electrodynamics (QED) [8], the quantum theory of electromagnetic interaction [7]. As an extension of relativistic quantum mechanics, it models not only electrons, but also their radiation fields [9]. Several spin-precession experiments have measured the Landé g factor of the muon which is proportional to the magnetic moment [8].

The first measurement of g for muons was made in 1957 by Garwin et. al. at the Nevis Cyclotron Laboratories of Columbia University [8]. A cyclotron was used to produce a positive muon beam formed from positive pions that decayed in flight. The beam was then stopped in a carbon target in a magnetic field. The value of g was determined to be $2.00 \pm 0.10$ [10]. A more accurate measurement was made at CERN by J. Bailey et. al. in 1979 [11]. Data collected in 1999 for the Muon (g-2) Collaboration at the Brookhaven Alternating Gradient Synchrotron, however, has made one of the most accurate measurements of g to date [12].

### 1.2 Purpose

The purpose of our experiment was to measure the magnetic moment of the muon using cosmic ray muons and a "tabletop" scale apparatus. This was accomplished by analyzing the positron emission of positive muons precessing in a known magnetic field. This idea was obtained from a paper written by C. Amsler which discussed a similar experiment carried out in 1974 at the Laboratory of High Energy Physics of the Swiss Federal Institute of Technology [13].

### 1.3 Changes to the Previous Experimental Design

The experiment described here used a similar apparatus to Amsler's with changes in solenoid design, detector setup, electronics, and triggers. Accompanying the description of these changes is a discussion of their advantages and disadvantages.

#### 1.3.1 Solenoid

The solenoid producing the magnetic field was very similar to Amsler's with a few minor differences. While our solenoid consisted of 1348 wire windings on a cardboard tube, Amsler's was only 1000 wire windings on a rectangular aluminum frame. His field was a little stronger than ours with a maximum field strength of 50 G compared to our 44 G maximum. The inhomogeneity of his field, which was $\pm 4\%$ from the average, was about 1% more uniform than ours. Inhomogeneity affects the precession of muons in the field. The more uniform the field, the more constant the muon precession rate will be, resulting in less systematic error.

Amsler's solenoid was slightly larger than ours in terms of total surface area, which could account for the larger uniform field region. While it was only 100 cm long compared to 136 cm, its sides measured 63 cm and 10 cm. Our solenoid had a diameter of 27 cm so even with our added length, the total surface area was more than 3,000 $cm^2$ smaller.

#### 1.3.2 Detector Arrangement

A more substantial difference between his experiment and ours was his detector setup. As seen in Fig. 1.1, Amsler stacked three plastic scintillators on top of each other to detect incident muons and placed a copper plate in between the middle scintillator and the bottom one to stop the muons. We used the same scintillator arrangement but made use of a thick center scintillator to stop the muons. The advantage of using a copper plate instead of relying on a thick scintillator to stop muons is that the copper will stop more muons. This would allow more data to be collected in a shorter period of time. This difference of course necessitated a slightly different electronic circuit for triggering and detecting the proper particles and emissions.

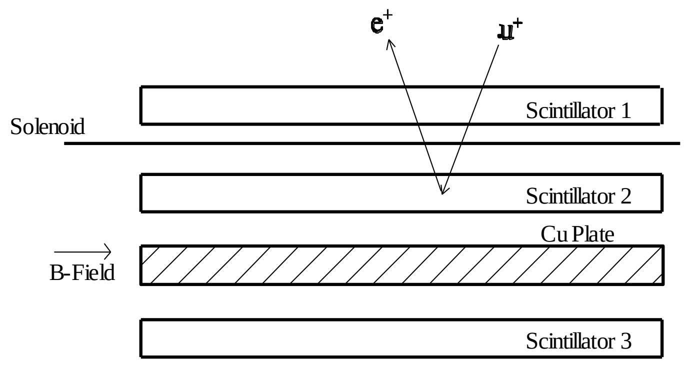


[Figure 1.1] This is a schematic diagram of Amsler's apparatus. Three plastic scintillators inside a solenoid detect incident muons, which precess in the magnetic field, as well as their positron emissions.

### 1.3.3 Triggers

Amsler's stopped muon trigger was produced by pulses from the top two scintillators but not the bottom one. This trigger was identical to ours, but Amsler used the same trigger to determine if a positron was ejected up when the muon decayed. Our decay trigger waited for a positron to be ejected down. This reduced systematic error, because two muons entering one right after the other would not be recorded as a decay.

### 1.3.4 Timing Calibration Technique

The last important difference between the two experiments was the timing calibration technique. Amsler used an oscilloscope and a quartz clock. He checked the time base of the oscilloscope with the clock. Our system was calibrated using a gate generator which produced known time delay between two pulses. These time delays allowed us to determine the timing calibration. This paper describes the experimental apparatus and procedures in detail, but first briefly introduces the theory motivating this experiment.

*Chapter 2*

# THEORY

## 2.1 Muon Characteristics

Muons are produced in the upper atmosphere in pion and kaon decay. Pions and kaons are mesons, i.e., hadrons consisting of only two quarks. When cosmic ray protons bombard nuclei in the upper atmosphere, they create primaries—particles created directly from nuclear interactions. The particles they decay into, such as muons, are called secondaries [2]. Pions and kaons are the most abundant primaries because they are the least massive hadrons and thus the easiest to create. Since pions are the most abundant particles produced, they are the primary producer of cosmic ray muons.

Since muons do not interact via the strong force, but only by gravity, the electromagnetic and weak forces, they are categorized as leptons. As such, they are very similar to electrons and can be thought of as massive electrons. Muons have a mass of 105.7 MeV/$c^2$, and are spin-½ particles with the magnetic moment [3]

$$\vec{\mu}_\mu = \frac{ge}{2m_\mu c}\vec{S} \tag{2-1}$$

Taking into account the mass difference, they have the same electromagnetic properties as electrons. Their large mass makes them unstable with a mean lifetime of about 2.2 μs, and their decay follows a purely leptonic scheme (≈100% of the time) [14]

$$\mu^{+} \rightarrow e^{+} + \nu_{e} + \bar{\nu}_{\mu} \tag{2-2}$$

$$\mu^{-} \rightarrow e^{-} + \bar{\nu}_{e} + \nu_{\mu} \tag{2-3}$$

## 2.2 Experimental Apparatus

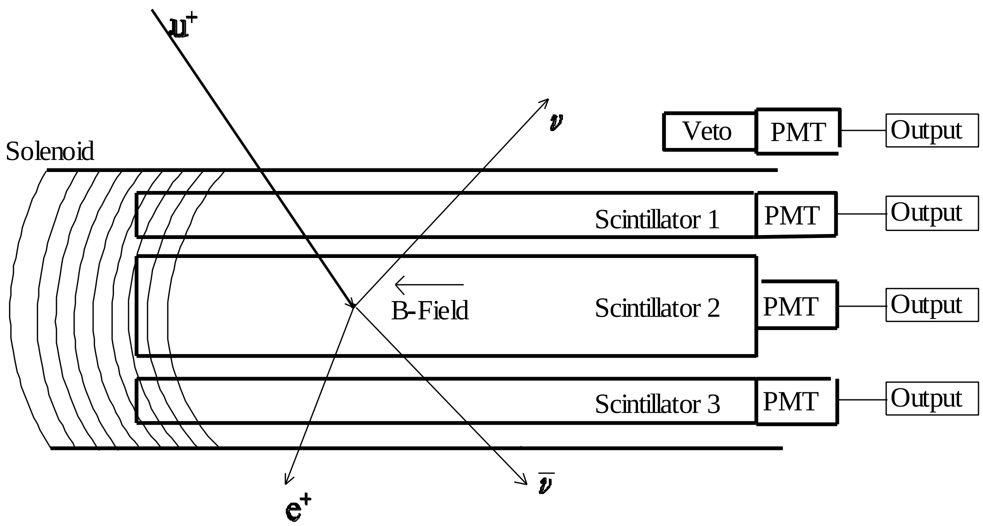


[Figure 2.1] This is a schematic diagram of the experimental apparatus. Three plastic scintillators inside a solenoid detect incident muons, which precess in the magnetic field, as well as their positron emissions.

This experiment measured the magnetic moment of the muon by recording the lifetimes of muons as their spins precessed in a uniform magnetic field. As seen in Fig. 2.1, there were three plastic scintillators inside a solenoid that produced a constant magnetic field. A smaller scintillator vetoed events from a non-uniform region of the field near the end of the solenoid. The outputs from the scintillators were analyzed by a logic circuit that will be discussed in detail later. The lifetimes of muons that stopped in the center scintillator in the uniform magnetic field and ejected a positron down through the bottom scintillator were recorded and plotted on a computer forming a decay curve. A decay rate equation was then fit to this curve.

As muons streamed through the apparatus, some were stopped in the center scintillator. Negative muons were quickly caught by nuclei in the scintillator causing them to decay much more rapidly than positive muons and are therefore not important for this experiment [13]. A stopped positive muon precessed in the magnetic field and decayed emitting a positron anti-parallel to its spin axis [8]. The time difference between a muon stopping in the center detector and ejecting a positron through the bottom scintillator was measured and recorded.

Coincident pulses from scintillators one and two, but not three and not the veto, indicated that a muon had stopped in the center detector in a uniform region of the field, and started a timer. Coincident pulses from scintillators two and three, but not one, that were received within 20 μs of the starting signal, indicated that the muon had decayed by emitting a positron downward. If no pulses were received within 20 μs of the first coincidence, then the event was considered an accidental coincidence.

### 2.3 Muon Precession

Since muons interact via the electromagnetic force, they respond strongly to magnetic fields. In fact, the expectation value of the muon's spin precessed at a rate proportional to the magnitude of the magnetic field [13]. The vector in Fig. 2.2 is the expectation value of the muon's spin. As the expectation value of the spin moves farther away from +y and closer to –y, the probability that the muon has $S_z = -\hbar/2$ is decreasing while the probability that it has $S_z = +\hbar/2$ is increasing. The precessional frequency of the expectation value is given by

$$\omega = g\frac{eH}{2m_\mu c} \qquad (2\text{-}4)$$

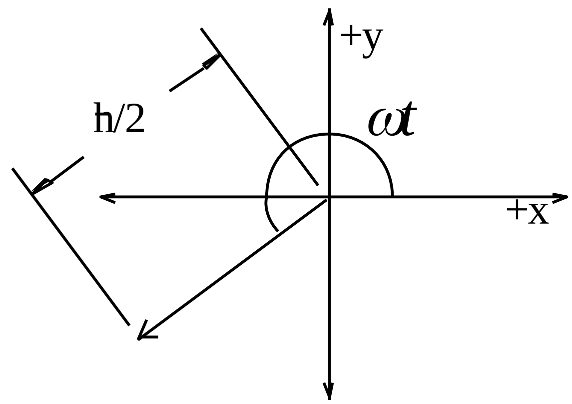


[Figure 2.2] This shows the precession of the expectation value of a muon's spin in a constant magnetic field. ħ/2 is the magnitude of the expectation value and ωt is precessional frequency.

where g is the Landé g factor, e is the charge of an electron, H is the magnetic field strength, $m_\mu$ is the muon mass, and c is the speed of light [3]. This is important because the spin direction determines the direction that the positron is ejected. Thus, the lifetime of a given muon determines the likelihood that the positron will be ejected upward or downward.

### 2.4 Muon Polarization

If muons arrived in the magnetic field with random polarizations, then they would eject their decay positrons randomly upward or downward. As I will discuss next, this is not the case, since they have a net polarization.

The polarization of cosmic ray muons arises from their origin in pion decay. Speeding towards Earth at nearly the speed light, pions decay producing muons about 99.99% of the time via

$$\pi^{\pm} \rightarrow \mu^{\pm} + \nu_\mu \qquad (2\text{-}5)\ [14]$$

In the pion rest frame, pions eject these muons in random directions. In the laboratory frame, however, pions flying towards the Earth eject the muons only forward or backward because the angles at which they were ejected in the rest frame are relativistically compressed. The direction of ejection determines the spin direction of the muon. Since most pions are coming from directly overhead, the muons generally arrive with either spin upward or spin downward. If the number of ejections forward was equal to the number of ejections backward, then the spin direction of incoming muons would be randomly up or down. However, since they are not equal, there is a net polarization of the arriving muons, i.e., there is a slightly preferred direction of spin, as a function of energy.

Zero polarization will only occur if the production spectrum is flat. However, since muon energies depend on the altitude and latitude at which the pions decayed, the spectrum is not flat, and thus, muons have a net polarization [13, 15]. Experiments have verified this as seen in Fig. 2.3.

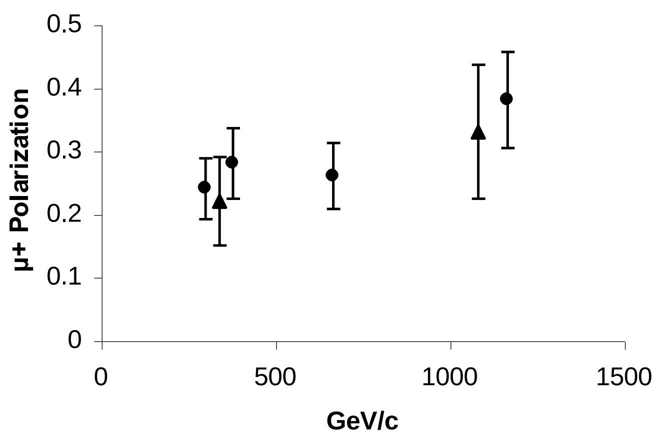

[Figure 2.3] A plot of positive muon polarization at sea level as a function of momentum according to Ref. [13].

This polarization is very important because it affects the decay rate of the muons precessing in the magnetic field. Recording only downward emissions yields a decay curve that is not a purely exponential. Rather, since the muons are slightly polarized, certain lifetimes are more likely to result in an emission downward resulting in a sinusoidal variation of the exponential decay curve.

### 2.5 Data Analysis

The magnetic moment of the muons can be determined by analyzing these decay rate data. The decay rate of muons is given by

$$R(t) = R_0 \exp\left(-\frac{t}{\tau}\right) + B \tag{2-6}$$

where τ, the mean lifetime, is about 2.2 μs; $R_0$ is the initial rate at $t = 0$; and B accounts for background events. However, to determine the average magnetic moment, the decay rate of muons that precessed in a constant magnetic field and ejected in a given direction must be analyzed as discussed earlier. This is given by

$$R(t) = R_0 \exp\left(-\frac{t}{\tau}\right)(1 + A\sin(\omega t + \delta)) + B \tag{2-7}$$

where A accounts for muon and positron acceptance angles and muon polarization, δ accounts for initial muon polarization direction, and B is the background rate [13]. From this equation, the angular speed of precession, ω, can be determined by

$$\omega = g\,\frac{eH}{2m_\mu c} \tag{2-4}$$

where g is the Landé g factor and

$$\vec{\mu}_\mu = \frac{ge}{2m_\mu c}\vec{S} \tag{2-1}$$

*Chapter 3*

APPARATUS

## 3.1 Tabletop Apparatus

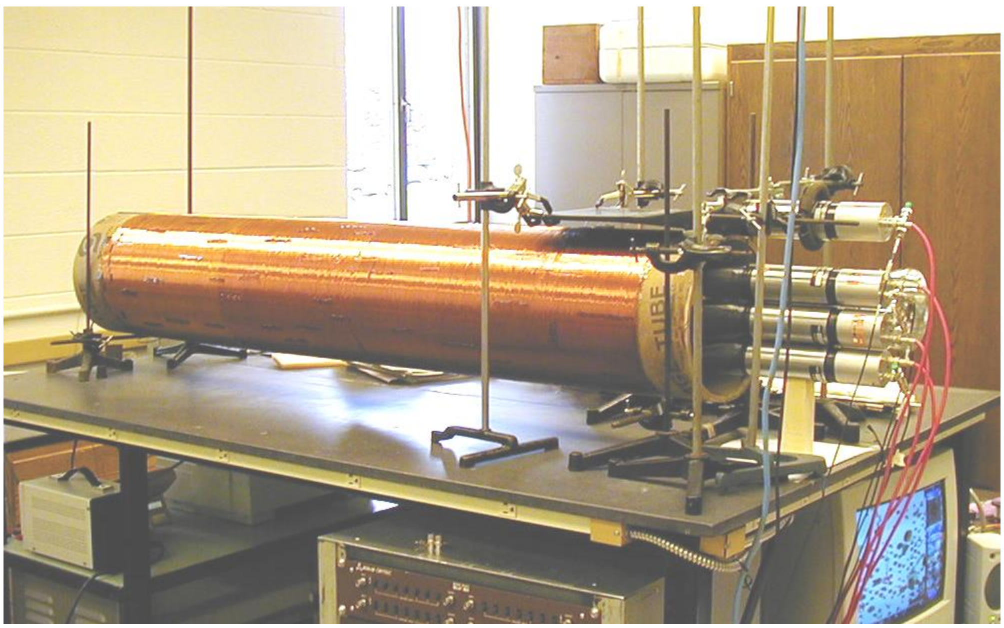


[Figure 3.1] This is a photograph of the experimental apparatus. The large solenoid produced the constant magnetic field the muons precessed in. The three scintillators inside the solenoid detected the muons and decay positrons. The small scintillator over the end of the solenoid vetoed events in the non-uniform region of the field.

As the title suggests, the experimental apparatus was designed to be small enough to fit on a table. Fig. 3.1 is a photograph of the apparatus. The three plastic scintillators used to detect muons and their emissions are shown as they rested inside the solenoid. The small plastic scintillator mounted over the end of the solenoid vetoed events that occurred outside the region of constant flux near the end of the solenoid.

### 3.2 Solenoid

The constant magnetic field needed for muon precession was provided by the large, 136 cm long by 27 cm diameter solenoid which is described in Appendix A. The magnetic field of the solenoid was a maximum of 44 G in the center. A field of 39 G, 10% below the maximum field, was decided on as the acceptable minimum. As seen from Fig. 3.2, this low value occurred twice—once at each end of the solenoid—demarcating the region of the solenoid which could be used for the experiment. The field within the specified tolerance spanned the 1-meter region between 0.4 m and 1.4 m on the plot with an average field strength of 42 G ± 5%.

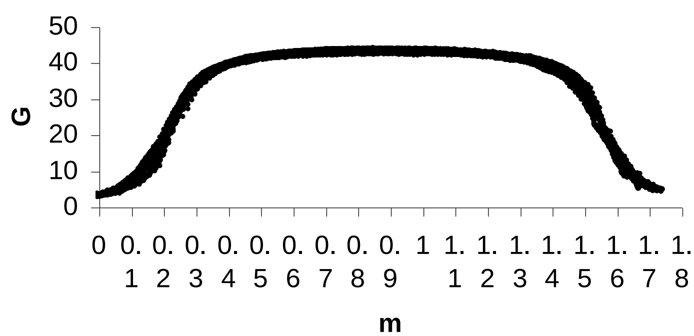


[Figure 3.2] This is a plot of the magnetic field strength of the solenoid as a function of position inside the solenoid.

### 3.3 Apparatus Components

Fig. 3.3 on page 16 is a diagram of the experimental apparatus and electronics. Plastic scintillators inside a large solenoid were used to detect incoming muons and positron emissions from muon decays. A fan was used for cooling to protect the scintillators form the ohmic heating in the solenoid. Scintillators are made from dense, black-coated plastic, which receive charged particles that ionize the plastic resulting in the emission of light pulses (see Appendix B). These pulses travel through the plastic and enter a light guide, which is attached to a photomultiplier tube. The photomultiplier tubes receive the light pulses and convert them to analog electrical pulses (see Appendix B), which are sent to the discriminators in the order received.

### 3.3.1 Scintillators

The apparatus used four Bicron BC-400 plastic scintillators. The thick scintillator (102.0 × 20.6 × 5.4 cm) was used to stop incident muons. It was within this scintillator that the muon precessions of interest took place. Two thinner scintillators (102.0 × 20.6 × 1.6 cm) were placed above and below the thick scintillator to detect incident muons and their decay positron emissions. As discussed previously, only positrons emitted downward were of interest. The Logic units discussed later identified muons that stopped in the thick scintillator and emitted positrons through the bottom scintillator.

The fourth scintillator was a small scintillator (21.0 × 20.5 × 1.0 cm) used to veto events occurring in the non-uniform region of the field. Originally, the three main scintillators were placed far enough inside the solenoid that this was not an issue. Unfortunately, however, the magnetic field was large enough to interfere with the operation of the photomultiplier tubes, even though they were protected with mu metal casings. To correct this, the scintillators were pulled out of the solenoid enough to reduce the magnetic flux through the photomultiplier tubes. Doing this however, meant that events occurring outside of the region of uniform field would be recorded. Placing a small scintillator over the unacceptable region allowed events occurring in this region to be eliminated.

### 3.3.2 Discriminators

The LeCroy 4608C discriminators received the analog electrical pulses from the photomultiplier tubes and analyzed them to discriminate between muon events and noise. Noise is produced from dark current in the photomultiplier tubes (see Appendix B) and background radiation. Real pulses exceed a minimum voltage threshold that noise pulses usually do not reach. For each real pulse received, the discriminators output a corresponding logic pulse to the logic units.

### 3.3.3 Logic Units

The LeCroy 365AL logic units determined when a muon stopped in scintillator 2 and if the muon ejected a positron downward when it decayed. The circuit consisted of two AND gates which looked for two distinct conditions—a starting coincidence and a stopping coincidence. Pulses from the AND gates were relayed to the Ortec 566 Time to Amplitude Converter (TAC) which measured the time difference between a starting coincidence and a stopping coincidence. One AND gate sent a pulse to the starting input of the TAC if it received a pulse from scintillator 1 and scintillator 2 but not from scintillator 3 or the veto. This meant that the muon stopped either in scintillator 2 in the uniform region of the field or in the region between scintillators 2 and 3. If the upper AND gate detected coincident pulses from scintillators 2 and 3 within 20 μs of the starting coincidence, but not from scintillator 1, a pulse was sent to the stopping input. This coincidence corresponded to a positron being emitted downward from the decay of the muon. If 20 μs elapsed without the stopping coincidence occurring, the TAC automatically reset and waited for another starting signal. If, as mentioned before, a muon stopped in the region between scintillators 2 and 3, the TAC would time out and reset even if it ejected downward because scintillator 2 would not register the decay required by the stopping coincidence.

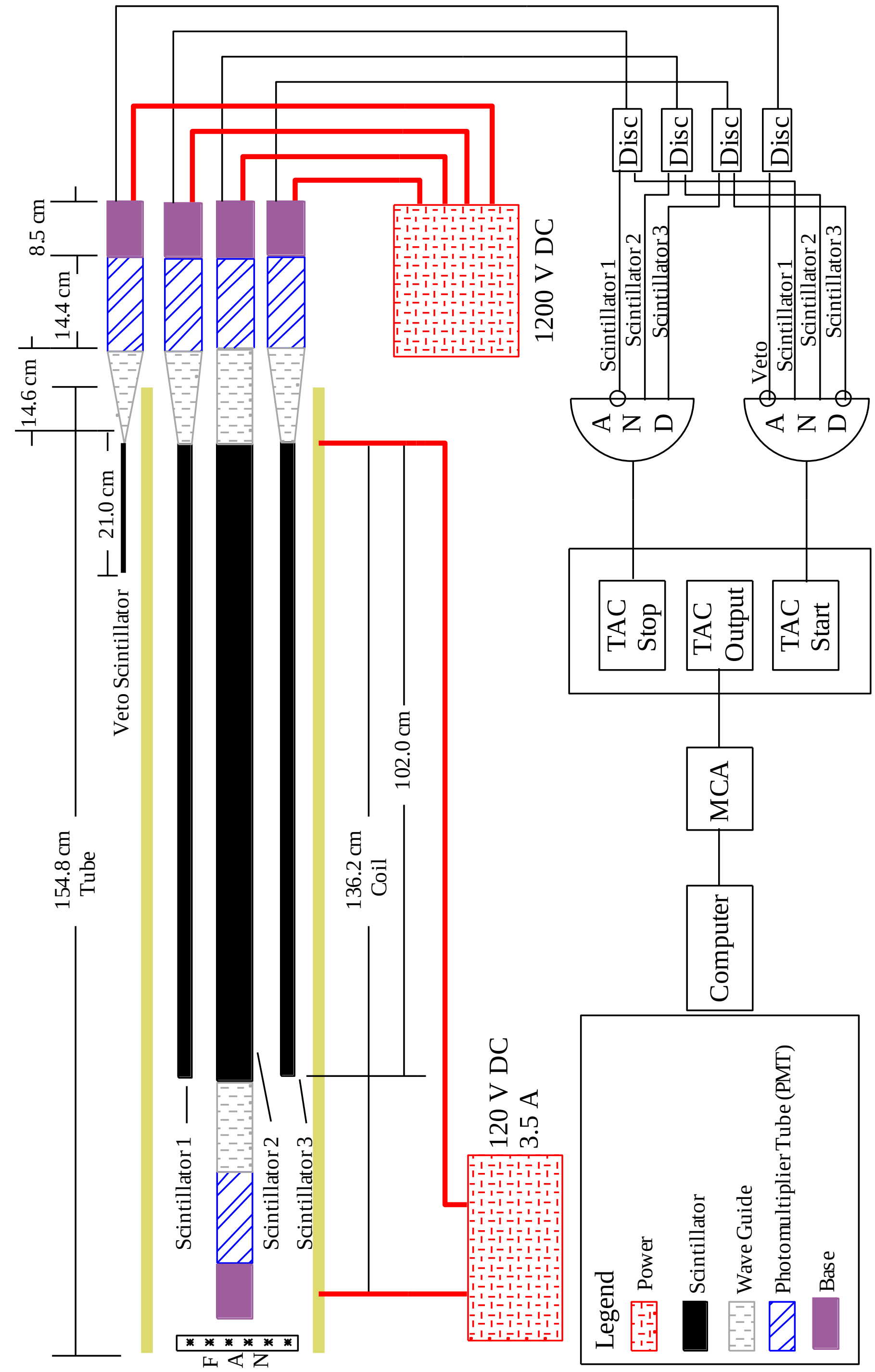


[Figure 3.3] This is a schematic diagram of the tabletop apparatus and electronics.

### 3.3.4 Time to Amplitude Converter and Multichannel Analyzer

When the logic circuit determined that a muon had entered the field and stopped in the thick scintillator, a pulse was sent to the TAC starting a timer. If the logic circuit then received pulses indicating that the muon had decayed and emitted a positron through the bottom scintillator, a second pulse was sent to the TAC to stop the timer. The TAC created an analog voltage pulse of magnitude proportional to the time difference (0-10 V) which was input to the AMPTEK MCA-8000A multichannel analyzer, which digitized the pulse and created a histogram in memory of the decay time. If a stopping coincidence was not identified by the logic circuit within 20 μs of a starting coincidence, the TAC simply reset itself and waited for a new start pulse. The value of 20 μs was chosen because it is considerably longer than the muon mean lifetime.

## 3.4 Timing Calibration

From the previous discussion, recall that certain lifetimes corresponded to certain histogram channels. Also recall that the computer simply recorded the number of events in each channel. Therefore, time calibration is necessary in order to interpret the data. This was done using a LeCroy 2323A programmable CAMAC dual gate generator (see Fig. 3.4). A single photomultiplier tube was connected to the discriminator. When a pulse arrived from the photomultiplier tube, the discriminator sent a logic pulse to the starting gate of the TAC and a second pulse to the gate generator. The gate generator in turn waited a known amount of time before sending a pulse to the stopping gate of the TAC. Thus, all events were placed in the same channel, corresponding to the delay time on the gate generator. This was done for several time delays and a linear calibration equation was determined.

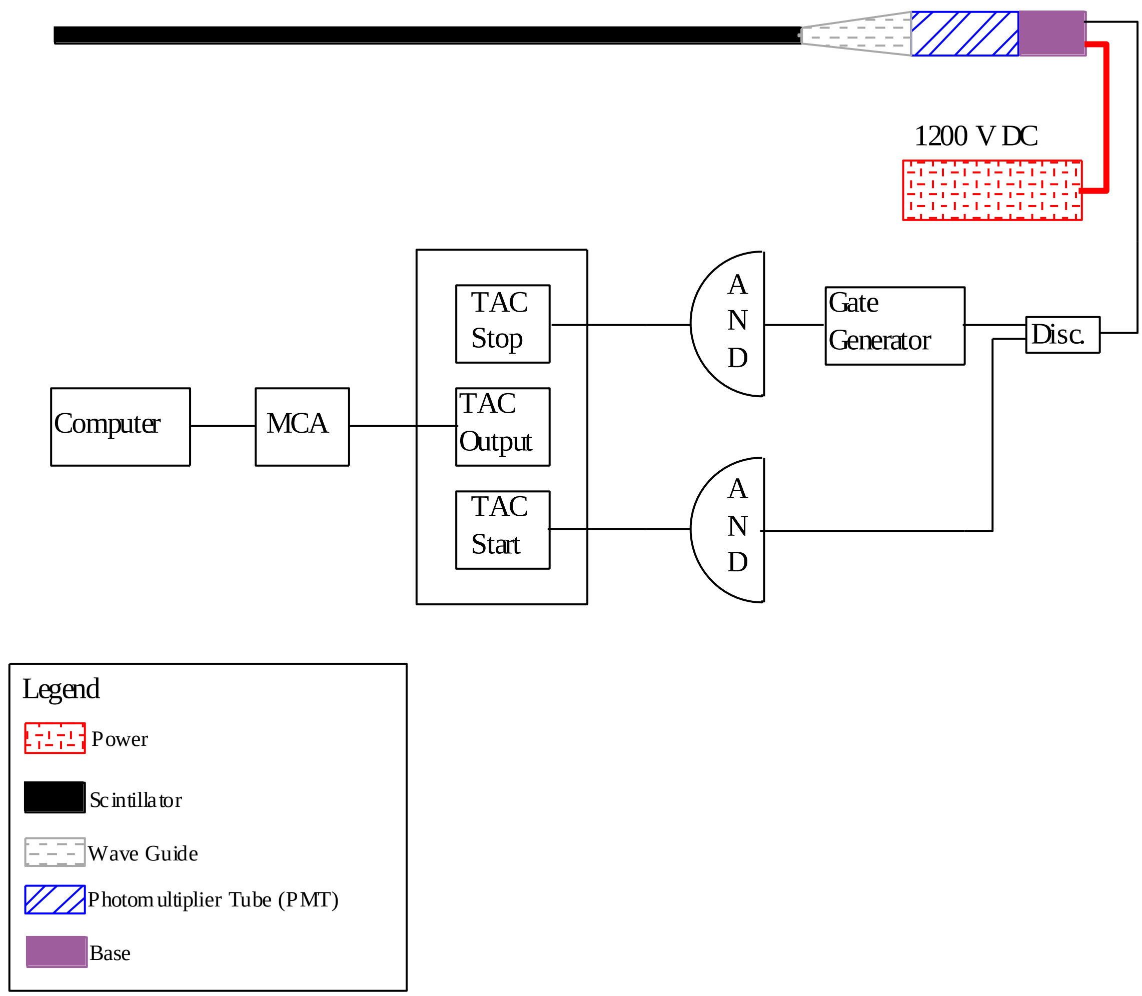


[Figure 3.4] This is a schematic diagram of the timing calibration circuit. A gate generator produced a selectable time delay between the start and stop of the TAC. Using the known times corresponding to measured channels, a linear calibration equation was obtained.

*Chapter 4*

# RESULTS AND CONCLUSION

A fit of Equations 2-6 and 2-7 to the experimental decay rate data (see Appendices C and D) yielded the results shown in Table I—the Landé g factor and the mean lifetime of the muon. As seen in Fig. 4.1 on the following page, the decay curve for muons with no magnetic field present was purely exponential. The decay curve for muons in a constant magnetic field however (Fig. 4.2), had a sinusoidal variation superimposed on the exponential decay because the lifetimes corresponding to the upward prominences on the curve were more likely to result in an emission downward due to precession.

[Table 4-I] This is a table of our experimental results and previously measured values for comparison.

| | |
|---|---|
| Muon Mean Lifetime | $\tau = 2.19 \pm 0.04$ μs |
| Previously Measured Value [14] | $\tau = 2.19703 \pm 0.00004$ μs |
| Landé g Factor | $g = 2.89 \pm 0.16$ |
| Previously Measured Value [12] | $g = 2.00233184 \pm 0.000000003$ |

As seen in Table 4-I, from the data collected without the magnetic field, we obtained the mean lifetime of the muon to be $\tau = 2.19 \pm 0.04$ μs. Comparing our measurement with others [10,11,14], we see good agreement, well within the experimental uncertainty. The data collected with the constant magnetic field yielded a Landé g factor of $g = 2.89 \pm 0.16$, which is somewhat higher than the values determined by Garwin et. al., J. Bailey et. al., and N. H. Brown et. al. [10,11,12].

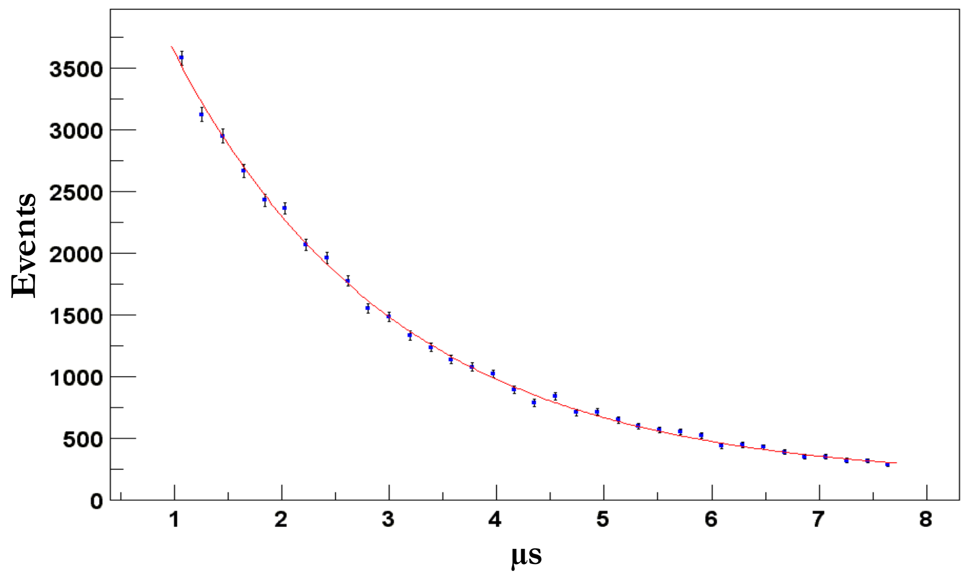


[Figure 4.1] This is a plot of the background data, i.e., data collected with no magnetic field present. The x-axis corresponds to the muon lifetime in μs and the y-axis corresponds to the number of events. The solid line is the fit of Equation (2-6).

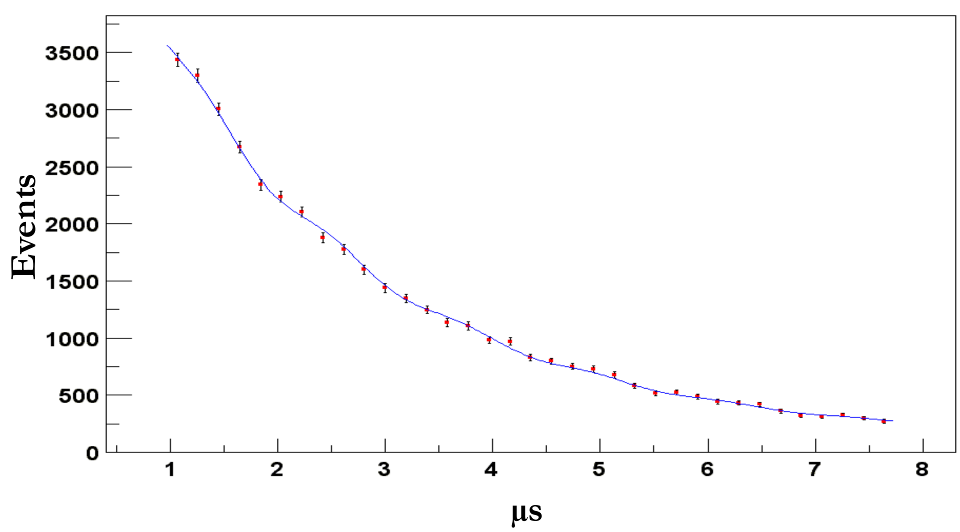


[Figure 4.2] This is a plot of the data with a 42 G ± 5% magnetic field present. The axes are the same as in Fig. 4.1. The solid line is a fit of Equation (2-7).

*Appendix A*

# SOLENOID DESIGN

As stated in Chapter 2, a constant magnetic field was necessary to carry out this experiment. This was provided by a large solenoid, which was large enough to accommodate the three plastic scintillators in Fig. 3.1. A 10-inch diameter Sonotube cardboard tube designed for pouring concrete footers was ideal for making such a solenoid. After cutting the tube to an appropriate length of about 1.5 m (a little longer than needed for the wire coil), 19-gauge copper magnet wire with enamel insulation was wrapped around and secured to the cardboard tube with epoxy.

Design of the solenoid and calculation of the magnetic field was done through trial and error, working within certain parameters. The strongest magnetic field possible given the physical limitations of our available wire and power source was the goal. The solenoid length decided on was 135 cm. Since 1039.4 wire turns yielded one meter of coil, 1.2 km of wire was needed to make a 135 cm coil. Given a resistance of 32.5 Ω for 1.2 km of 19 gauge wire, it was decided that about 50 G would be the maximum field since 124.5 V would be needed for a current of 3.8 A. Higher currents would require too high a power output and require a larger power supply than was readily available.

When finished, the solenoid consisted of a 155 cm long by 27 cm diameter cardboard tube around which was wrapped about 1.2 km of 19 gauge copper magnet wire. The wire was wrapped a total of 1,348 times forming a 136 cm long coil around the tube. A Bud Radio Corp. power supply produced a 3.5 A current generating a fairly constant magnetic field of 42 G ± 5% in a 1 m region of the tube (see Fig. 3.2). The resistance of the solenoid required 120 V for 3.5 A of current, resulting in 420 W of ohmic heating.

The resistance of the coil and maximum voltage of the power supply were the main factors that limited the magnetic field strength to 42 G. The operating resistance, which is given by $R = \frac{V}{I}$, was about 34.3 Ω. The room temperature resistance of the solenoid was 31.2 Ω, so the resistance did increase with the temperature of the coil to some degree. The small fan shown in Fig. 3.3 was used to circulate air through the inside of the coil to prevent overheating.

Once built, the solenoid's magnetic field was mapped in order to determine the actual field strength as a function of position. A wooden cart carrying a Vernier Software MG-DIN magnetic field sensor was moved down the core of the solenoid on a track at various heights to map the field. An origin was picked for the cart and a string attached to it, which was also attached to a PASCO scientific CI-6625 rotary motion sensor. The cart was then moved through the solenoid—the probe measuring the magnetic field and the motion sensor measuring the distance traversed. Logger Pro software was used to plot this data on two axes giving us a graph of the magnetic field as a function of position within the solenoid. Repeating this procedure at various heights within the solenoid verified that the field did not vary much with respect to radial distance from the solenoid axis (see Fig. 3.2).

*Appendix B*

## SCINTILLATOR AND PHOTOMULTIPLIER TUBE OPERATION

Plastic scintillators, which are a type of organic scintillator, are made of materials belonging to the class of aromatic compounds, i.e., compounds consisting of planar molecules made of benzoid rings. Appropriate compounds are combined in solution to form organic scintillators. The most abundant compound is called the solvent and the others solutes. While it is evident that this applies to liquid scintillators, it also applies to plastic scintillators, which are a solid solution [16].

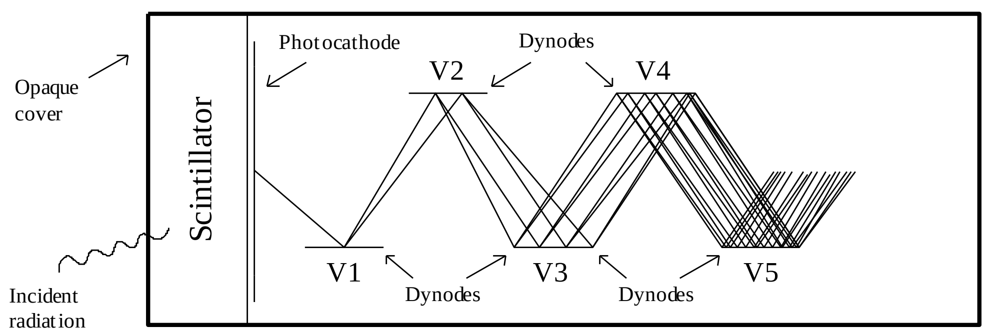


[Figure B.1] This is a schematic diagram of a photomultiplier tube coupled to a scintillator. Light pulses from the scintillator cause the photocathode to emit electrons which are guided from dynode to dynode producing more electrons in an avalanche. The electrons are collected by an anode which transmits the current pulse to be analyzed by other electronics.

Light pulses are produced in organic scintillators from molecular transitions that occur when the compounds are exposed to ionizing radiation. As seen in Fig.

B.1, light from the scintillator enters an evacuated glass tube striking a photocathode at the entrance. These electron pulses are very rapidly (≈1 ns) amplified by a factor of $10^6$ or more by the dynodes in the photomultiplier tubes. The photocathode emits electrons which are guided by a strong electric field towards a dynode. The dynode is coated with a material that emits secondary electrons when the electrons from the photocathode impinge upon it. These electrons are then guided towards the next dynode and subsequently towards the rest. Each dynode has an 80–120 V higher positive voltage (higher) than the one before, and therefore each electron is accelerated between dynodes knocking out more electrons each time in an avalanche. A photomultiplier tube may have as many as 15 dynodes. The electrons from the final dynode are collected by an anode at the end of the tube. The change in the current pulse produced is proportional to the intensity of the light pulse received which in turn is proportional to the energy of the incident ionizing radiation. This current pulse is analyzed by the electronics discussed in Chapter 3 [16].

Dark current from the photomultipliers tubes must be considered. It is a product of thermionic emission of electrons from the photocathode and dynodes. As mentioned in chapter 3, photomultiplier tubes are also sensitive to magnetic fields because the electrons traveling down the dynode chain will be deflected by them. For this reason, photomultiplier tubes are usually encased in mu metal. In our experiment, however, the magnetic field lines were along the axis of the photomultiplier tubes, rendering the mu metal shields ineffective [16].

*Appendix C*

# BACKGROUND DATA

The following data were collected with no magnetic field present so the muon decay rate as well as background rate of accidental events could be determined and compared to the data with the magnetic field present. The data were fit to Equation (2-6).

[Table C-I] This is a table of the background data. For each MCA channel the number of events is given. For this measurement, the magnetic field was removed.

| Channel | Events | Channel | Events | Channel | Events | Channel | Events |
|---|---|---|---|---|---|---|---|
| 1 | 0 | 23 | 485 | 45 | 385 | 67 | 358 |
| 2 | 0 | 24 | 479 | 46 | 410 | 68 | 366 |
| 3 | 0 | 25 | 482 | 47 | 397 | 69 | 347 |
| 4 | 0 | 26 | 485 | 48 | 404 | 70 | 336 |
| 5 | 0 | 27 | 467 | 49 | 382 | 71 | 340 |
| 6 | 0 | 28 | 495 | 50 | 435 | 72 | 351 |
| 7 | 0 | 29 | 491 | 51 | 402 | 73 | 341 |
| 8 | 0 | 30 | 477 | 52 | 417 | 74 | 308 |
| 9 | 0 | 31 | 463 | 53 | 358 | 75 | 294 |
| 10 | 3 | 32 | 458 | 54 | 379 | 76 | 327 |
| 11 | 516 | 33 | 484 | 55 | 394 | 77 | 310 |
| 12 | 572 | 34 | 474 | 56 | 369 | 78 | 296 |
| 13 | 545 | 35 | 458 | 57 | 395 | 79 | 305 |
| 14 | 596 | 36 | 461 | 58 | 383 | 80 | 286 |
| 15 | 533 | 37 | 445 | 59 | 386 | 81 | 304 |
| 16 | 509 | 38 | 414 | 60 | 362 | 82 | 323 |
| 17 | 528 | 39 | 430 | 61 | 379 | 83 | 323 |
| 18 | 542 | 40 | 453 | 62 | 359 | 84 | 288 |
| 19 | 541 | 41 | 389 | 63 | 361 | 85 | 306 |
| 20 | 547 | 42 | 432 | 64 | 402 | 86 | 296 |
| 21 | 539 | 43 | 450 | 65 | 357 | 87 | 273 |
| 22 | 526 | 44 | 438 | 66 | 353 | 88 | 290 |

| | | | | | | | |
|---|---|---|---|---|---|---|---|
| 89 | 287 | 135 | 232 | 181 | 137 | 227 | 98 |
| 90 | 286 | 136 | 173 | 182 | 130 | 228 | 75 |
| 91 | 277 | 137 | 199 | 183 | 124 | 229 | 85 |
| 92 | 281 | 138 | 191 | 184 | 126 | 230 | 81 |
| 93 | 297 | 139 | 183 | 185 | 107 | 231 | 88 |
| 94 | 274 | 140 | 181 | 186 | 110 | 232 | 84 |
| 95 | 271 | 141 | 186 | 187 | 134 | 233 | 81 |
| 96 | 274 | 142 | 183 | 188 | 124 | 234 | 68 |
| 97 | 253 | 143 | 197 | 189 | 128 | 235 | 108 |
| 98 | 231 | 144 | 178 | 190 | 116 | 236 | 76 |
| 99 | 276 | 145 | 180 | 191 | 137 | 237 | 78 |
| 100 | 248 | 146 | 162 | 192 | 109 | 238 | 76 |
| 101 | 262 | 147 | 159 | 193 | 124 | 239 | 71 |
| 102 | 278 | 148 | 169 | 194 | 102 | 240 | 78 |
| 103 | 276 | 149 | 167 | 195 | 102 | 241 | 68 |
| 104 | 280 | 150 | 202 | 196 | 116 | 242 | 101 |
| 105 | 238 | 151 | 176 | 197 | 102 | 243 | 83 |
| 106 | 221 | 152 | 155 | 198 | 135 | 244 | 93 |
| 107 | 241 | 153 | 147 | 199 | 123 | 245 | 63 |
| 108 | 232 | 154 | 165 | 200 | 109 | 246 | 84 |
| 109 | 225 | 155 | 172 | 201 | 117 | 247 | 90 |
| 110 | 207 | 156 | 133 | 202 | 124 | 248 | 81 |
| 111 | 232 | 157 | 138 | 203 | 95 | 249 | 82 |
| 112 | 261 | 158 | 143 | 204 | 139 | 250 | 96 |
| 113 | 275 | 159 | 156 | 205 | 100 | 251 | 67 |
| 114 | 240 | 160 | 166 | 206 | 107 | 252 | 71 |
| 115 | 220 | 161 | 178 | 207 | 96 | 253 | 57 |
| 116 | 231 | 162 | 141 | 208 | 106 | 254 | 76 |
| 117 | 266 | 163 | 158 | 209 | 103 | 255 | 74 |
| 118 | 225 | 164 | 162 | 210 | 114 | 256 | 69 |
| 119 | 246 | 165 | 173 | 211 | 94 | 257 | 68 |
| 120 | 191 | 166 | 155 | 212 | 107 | 258 | 72 |
| 121 | 208 | 167 | 132 | 213 | 111 | 259 | 80 |
| 122 | 178 | 168 | 143 | 214 | 89 | 260 | 72 |
| 123 | 243 | 169 | 127 | 215 | 122 | 261 | 71 |
| 124 | 196 | 170 | 162 | 216 | 110 | 262 | 75 |
| 125 | 199 | 171 | 134 | 217 | 93 | 263 | 65 |
| 126 | 218 | 172 | 150 | 218 | 110 | 264 | 67 |
| 127 | 208 | 173 | 127 | 219 | 95 | 265 | 73 |
| 128 | 215 | 174 | 135 | 220 | 99 | 266 | 81 |
| 129 | 195 | 175 | 138 | 221 | 85 | 267 | 75 |
| 130 | 200 | 176 | 139 | 222 | 90 | 268 | 75 |
| 131 | 213 | 177 | 126 | 223 | 96 | 269 | 73 |
| 132 | 206 | 178 | 137 | 224 | 100 | 270 | 56 |
| 133 | 202 | 179 | 130 | 225 | 94 | 271 | 75 |
| 134 | 210 | 180 | 113 | 226 | 87 | 272 | 68 |

| | | | | | | | |
|---|---|---|---|---|---|---|---|
| 273 | 66 | 319 | 46 | 365 | 36 | 411 | 33 |
| 274 | 72 | 320 | 49 | 366 | 33 | 412 | 31 |
| 275 | 71 | 321 | 52 | 367 | 32 | 413 | 32 |
| 276 | 65 | 322 | 36 | 368 | 39 | 414 | 26 |
| 277 | 67 | 323 | 52 | 369 | 41 | 415 | 25 |
| 278 | 59 | 324 | 49 | 370 | 34 | 416 | 24 |
| 279 | 62 | 325 | 54 | 371 | 32 | 417 | 34 |
| 280 | 68 | 326 | 42 | 372 | 39 | 418 | 38 |
| 281 | 50 | 327 | 43 | 373 | 37 | 419 | 29 |
| 282 | 57 | 328 | 47 | 374 | 36 | 420 | 22 |
| 283 | 57 | 329 | 42 | 375 | 39 | 421 | 30 |
| 284 | 53 | 330 | 39 | 376 | 35 | 422 | 33 |
| 285 | 66 | 331 | 34 | 377 | 32 | 423 | 27 |
| 286 | 56 | 332 | 50 | 378 | 31 | 424 | 23 |
| 287 | 76 | 333 | 53 | 379 | 40 | 425 | 25 |
| 288 | 64 | 334 | 40 | 380 | 30 | 426 | 25 |
| 289 | 64 | 335 | 39 | 381 | 30 | 427 | 29 |
| 290 | 57 | 336 | 45 | 382 | 36 | 428 | 19 |
| 291 | 48 | 337 | 47 | 383 | 28 | 429 | 24 |
| 292 | 58 | 338 | 42 | 384 | 37 | 430 | 25 |
| 293 | 58 | 339 | 46 | 385 | 33 | 431 | 23 |
| 294 | 63 | 340 | 42 | 386 | 40 | 432 | 32 |
| 295 | 51 | 341 | 42 | 387 | 36 | 433 | 30 |
| 296 | 66 | 342 | 48 | 388 | 32 | 434 | 22 |
| 297 | 49 | 343 | 35 | 389 | 27 | 435 | 26 |
| 298 | 69 | 344 | 38 | 390 | 20 | 436 | 24 |
| 299 | 50 | 345 | 46 | 391 | 32 | 437 | 18 |
| 300 | 57 | 346 | 43 | 392 | 30 | 438 | 25 |
| 301 | 46 | 347 | 31 | 393 | 42 | 439 | 27 |
| 302 | 61 | 348 | 51 | 394 | 33 | 440 | 17 |
| 303 | 74 | 349 | 42 | 395 | 28 | 441 | 17 |
| 304 | 57 | 350 | 53 | 396 | 30 | 442 | 17 |
| 305 | 49 | 351 | 42 | 397 | 26 | 443 | 25 |
| 306 | 41 | 352 | 28 | 398 | 35 | 444 | 35 |
| 307 | 52 | 353 | 48 | 399 | 41 | 445 | 22 |
| 308 | 43 | 354 | 49 | 400 | 25 | 446 | 25 |
| 309 | 49 | 355 | 52 | 401 | 27 | 447 | 25 |
| 310 | 57 | 356 | 35 | 402 | 34 | 448 | 20 |
| 311 | 71 | 357 | 42 | 403 | 25 | 449 | 23 |
| 312 | 51 | 358 | 41 | 404 | 26 | 450 | 23 |
| 313 | 49 | 359 | 35 | 405 | 23 | 451 | 30 |
| 314 | 69 | 360 | 25 | 406 | 29 | 452 | 24 |
| 315 | 57 | 361 | 34 | 407 | 29 | 453 | 18 |
| 316 | 40 | 362 | 46 | 408 | 29 | 454 | 23 |
| 317 | 47 | 363 | 18 | 409 | 33 | 455 | 26 |
| 318 | 65 | 364 | 39 | 410 | 28 | 456 | 22 |

| | | | | | | | |
|---|---|---|---|---|---|---|---|
| 457 | 27 | 468 | 23 | 479 | 24 | 490 | 22 |
| 458 | 33 | 469 | 29 | 480 | 18 | 491 | 26 |
| 459 | 22 | 470 | 25 | 481 | 24 | 492 | 21 |
| 460 | 26 | 471 | 19 | 482 | 22 | 493 | 21 |
| 461 | 28 | 472 | 27 | 483 | 19 | 494 | 22 |
| 462 | 17 | 473 | 33 | 484 | 21 | 495 | 17 |
| 463 | 25 | 474 | 18 | 485 | 27 | 496 | 20 |
| 464 | 32 | 475 | 23 | 486 | 21 | **Total Number of Events** | 67761 |
| 465 | 30 | 476 | 26 | 487 | 24 | | |
| 466 | 21 | 477 | 23 | 488 | 25 | | |
| 467 | 23 | 478 | 21 | 489 | 22 | | |

*Appendix D*

## MAGNETIC FIELD PRECESSIONAL DATA

The following data were collected with a 42 G ± 5% magnetic field present so the effect of the muons' spin precession in the field could be seen in the decay rate. The data were fit to Equation (2-7).

[Table D-I] This is a table of the data with a 42 G ± 5% magnetic field present. For each MCA channel the number of events is given.

| Channel | Events | Channel | Events | Channel | Events | Channel | Events |
|---|---|---|---|---|---|---|---|
| 1 | 0 | 25 | 498 | 49 | 434 | 73 | 320 |
| 2 | 0 | 26 | 492 | 50 | 370 | 74 | 329 |
| 3 | 2 | 27 | 494 | 51 | 402 | 75 | 328 |
| 4 | 0 | 28 | 534 | 52 | 380 | 76 | 315 |
| 5 | 1 | 29 | 469 | 53 | 362 | 77 | 340 |
| 6 | 3 | 30 | 473 | 54 | 368 | 78 | 372 |
| 7 | 1 | 31 | 482 | 55 | 377 | 79 | 330 |
| 8 | 4 | 32 | 488 | 56 | 372 | 80 | 313 |
| 9 | 2 | 33 | 487 | 57 | 364 | 81 | 297 |
| 10 | 65 | 34 | 457 | 58 | 397 | 82 | 315 |
| 11 | 583 | 35 | 478 | 59 | 366 | 83 | 289 |
| 12 | 636 | 36 | 504 | 60 | 340 | 84 | 310 |
| 13 | 584 | 37 | 424 | 61 | 331 | 85 | 315 |
| 14 | 583 | 38 | 444 | 62 | 374 | 86 | 336 |
| 15 | 597 | 39 | 439 | 63 | 334 | 87 | 308 |
| 16 | 563 | 40 | 459 | 64 | 338 | 88 | 283 |
| 17 | 525 | 41 | 455 | 65 | 327 | 89 | 288 |
| 18 | 562 | 42 | 416 | 66 | 362 | 90 | 272 |
| 19 | 561 | 43 | 417 | 67 | 332 | 91 | 288 |
| 20 | 550 | 44 | 432 | 68 | 331 | 92 | 276 |
| 21 | 518 | 45 | 389 | 69 | 349 | 93 | 294 |
| 22 | 558 | 46 | 444 | 70 | 331 | 94 | 253 |
| 23 | 537 | 47 | 425 | 71 | 361 | 95 | 273 |
| 24 | 539 | 48 | 425 | 72 | 352 | 96 | 272 |

| | | | | | | | |
|---|---|---|---|---|---|---|---|
| 97 | 265 | 143 | 192 | 189 | 132 | 235 | 99 |
| 98 | 272 | 144 | 192 | 190 | 117 | 236 | 86 |
| 99 | 248 | 145 | 183 | 191 | 139 | 237 | 74 |
| 100 | 234 | 146 | 166 | 192 | 112 | 238 | 101 |
| 101 | 286 | 147 | 195 | 193 | 92 | 239 | 81 |
| 102 | 240 | 148 | 155 | 194 | 110 | 240 | 77 |
| 103 | 209 | 149 | 164 | 195 | 132 | 241 | 74 |
| 104 | 265 | 150 | 170 | 196 | 126 | 242 | 79 |
| 105 | 228 | 151 | 188 | 197 | 110 | 243 | 80 |
| 106 | 219 | 152 | 180 | 198 | 101 | 244 | 80 |
| 107 | 246 | 153 | 166 | 199 | 115 | 245 | 70 |
| 108 | 220 | 154 | 190 | 200 | 112 | 246 | 102 |
| 109 | 249 | 155 | 149 | 201 | 126 | 247 | 86 |
| 110 | 230 | 156 | 155 | 202 | 103 | 248 | 77 |
| 111 | 235 | 157 | 164 | 203 | 116 | 249 | 87 |
| 112 | 239 | 158 | 150 | 204 | 120 | 250 | 73 |
| 113 | 238 | 159 | 154 | 205 | 123 | 251 | 63 |
| 114 | 241 | 160 | 144 | 206 | 114 | 252 | 82 |
| 115 | 228 | 161 | 148 | 207 | 106 | 253 | 73 |
| 116 | 214 | 162 | 146 | 208 | 109 | 254 | 76 |
| 117 | 215 | 163 | 160 | 209 | 120 | 255 | 77 |
| 118 | 236 | 164 | 137 | 210 | 93 | 256 | 79 |
| 119 | 207 | 165 | 149 | 211 | 102 | 257 | 72 |
| 120 | 206 | 166 | 131 | 212 | 85 | 258 | 76 |
| 121 | 213 | 167 | 145 | 213 | 115 | 259 | 83 |
| 122 | 204 | 168 | 127 | 214 | 118 | 260 | 50 |
| 123 | 215 | 169 | 157 | 215 | 109 | 261 | 85 |
| 124 | 208 | 170 | 151 | 216 | 92 | 262 | 94 |
| 125 | 215 | 171 | 135 | 217 | 81 | 263 | 79 |
| 126 | 234 | 172 | 154 | 218 | 94 | 264 | 80 |
| 127 | 194 | 173 | 139 | 219 | 86 | 265 | 69 |
| 128 | 211 | 174 | 140 | 220 | 93 | 266 | 56 |
| 129 | 202 | 175 | 138 | 221 | 108 | 267 | 65 |
| 130 | 215 | 176 | 125 | 222 | 102 | 268 | 77 |
| 131 | 207 | 177 | 130 | 223 | 102 | 269 | 79 |
| 132 | 193 | 178 | 122 | 224 | 103 | 270 | 59 |
| 133 | 184 | 179 | 139 | 225 | 86 | 271 | 70 |
| 134 | 189 | 180 | 125 | 226 | 115 | 272 | 54 |
| 135 | 187 | 181 | 133 | 227 | 105 | 273 | 70 |
| 136 | 190 | 182 | 138 | 228 | 98 | 274 | 56 |
| 137 | 181 | 183 | 110 | 229 | 84 | 275 | 78 |
| 138 | 196 | 184 | 127 | 230 | 77 | 276 | 75 |
| 139 | 199 | 185 | 122 | 231 | 99 | 277 | 58 |
| 140 | 180 | 186 | 124 | 232 | 77 | 278 | 83 |
| 141 | 176 | 187 | 119 | 233 | 81 | 279 | 67 |
| 142 | 170 | 188 | 120 | 234 | 80 | 280 | 70 |

| | | | | | | | |
|---|---|---|---|---|---|---|---|
| 281 | 66 | 327 | 44 | 373 | 24 | 419 | 26 |
| 282 | 65 | 328 | 41 | 374 | 31 | 420 | 28 |
| 283 | 62 | 329 | 50 | 375 | 36 | 421 | 23 |
| 284 | 71 | 330 | 43 | 376 | 28 | 422 | 24 |
| 285 | 45 | 331 | 38 | 377 | 31 | 423 | 17 |
| 286 | 63 | 332 | 33 | 378 | 36 | 424 | 17 |
| 287 | 54 | 333 | 44 | 379 | 27 | 425 | 26 |
| 288 | 61 | 334 | 54 | 380 | 34 | 426 | 21 |
| 289 | 56 | 335 | 44 | 381 | 32 | 427 | 28 |
| 290 | 57 | 336 | 44 | 382 | 34 | 428 | 29 |
| 291 | 47 | 337 | 42 | 383 | 40 | 429 | 20 |
| 292 | 57 | 338 | 48 | 384 | 32 | 430 | 31 |
| 293 | 51 | 339 | 45 | 385 | 40 | 431 | 28 |
| 294 | 57 | 340 | 38 | 386 | 28 | 432 | 17 |
| 295 | 48 | 341 | 40 | 387 | 32 | 433 | 29 |
| 296 | 60 | 342 | 42 | 388 | 31 | 434 | 30 |
| 297 | 42 | 343 | 42 | 389 | 28 | 435 | 18 |
| 298 | 46 | 344 | 34 | 390 | 29 | 436 | 19 |
| 299 | 64 | 345 | 41 | 391 | 33 | 437 | 24 |
| 300 | 47 | 346 | 40 | 392 | 36 | 438 | 19 |
| 301 | 44 | 347 | 38 | 393 | 32 | 439 | 35 |
| 302 | 42 | 348 | 54 | 394 | 25 | 440 | 28 |
| 303 | 64 | 349 | 48 | 395 | 27 | 441 | 32 |
| 304 | 55 | 350 | 36 | 396 | 30 | 442 | 24 |
| 305 | 45 | 351 | 44 | 397 | 27 | 443 | 25 |
| 306 | 51 | 352 | 40 | 398 | 30 | 444 | 24 |
| 307 | 57 | 353 | 35 | 399 | 26 | 445 | 34 |
| 308 | 55 | 354 | 39 | 400 | 28 | 446 | 22 |
| 309 | 60 | 355 | 26 | 401 | 36 | 447 | 34 |
| 310 | 42 | 356 | 30 | 402 | 30 | 448 | 18 |
| 311 | 51 | 357 | 42 | 403 | 29 | 449 | 25 |
| 312 | 52 | 358 | 39 | 404 | 26 | 450 | 25 |
| 313 | 46 | 359 | 25 | 405 | 25 | 451 | 21 |
| 314 | 46 | 360 | 37 | 406 | 28 | 452 | 24 |
| 315 | 60 | 361 | 47 | 407 | 23 | 453 | 20 |
| 316 | 43 | 362 | 36 | 408 | 38 | 454 | 23 |
| 317 | 51 | 363 | 35 | 409 | 24 | 455 | 27 |
| 318 | 41 | 364 | 34 | 410 | 23 | 456 | 30 |
| 319 | 56 | 365 | 25 | 411 | 26 | 457 | 28 |
| 320 | 47 | 366 | 31 | 412 | 21 | 458 | 19 |
| 321 | 48 | 367 | 32 | 413 | 30 | 459 | 22 |
| 322 | 41 | 368 | 36 | 414 | 36 | 460 | 28 |
| 323 | 58 | 369 | 25 | 415 | 37 | 461 | 23 |
| 324 | 48 | 370 | 32 | 416 | 43 | 462 | 20 |
| 325 | 37 | 371 | 36 | 417 | 27 | 463 | 26 |
| 326 | 46 | 372 | 33 | 418 | 38 | 464 | 24 |

| | | | | | | | |
|---|---|---|---|---|---|---|---|
| 465 | 23 | 474 | 27 | 483 | 20 | 492 | 19 |
| 466 | 25 | 475 | 19 | 484 | 26 | 493 | 29 |
| 467 | 16 | 476 | 29 | 485 | 21 | 494 | 35 |
| 468 | 26 | 477 | 21 | 486 | 13 | 495 | 19 |
| 469 | 22 | 478 | 23 | 487 | 22 | 496 | 20 |
| 470 | 18 | 479 | 24 | 488 | 19 | **Total Number of Events** | 68133 |
| 471 | 26 | 480 | 17 | 489 | 20 | | |
| 472 | 21 | 481 | 26 | 490 | 15 | | |
| 473 | 29 | 482 | 29 | 491 | 14 | | |

## References


[1] C. D. Anderson, S. H. Neddermeyer. *Phys. Rev.* **50**, 236 (1936); **51**, 884 (1937); **54**, 88 (1938).

[2] A. O. Weissenberg. *Muons*. American Elsevier Publishing Company, Inc., New York, 1967.

[3] E. G. Segrè. *Nuclei and Particles*. W. A. Benjamin, Inc., New York, 1965.

[4] M. Conversi, et. al. *Phys. Rev.* **68**, 232 (1945); **71**, 209 (1947).

[5] C. G. Lattes, et. al. *Nature, Lond.* **159**, 694 (1947).

[6] C. G. Lattes, et. al. *Nature, Lond.*, **160**, 453, 486 (1947).

[7] J. R. Taylor, C. D. Zafiratos. *Modern Physics for Scientists and Engineers*. Prentice-Hall, Inc., New Jersey, 1991.

[8] J. S. Townsend. *A Modern Approach to Quantum Mechanics*. McGraw-Hill, Inc., 1992.

[9] H. Kroemer. *Quantum Mechanics for Engineering, Materials Science, and Applied Physics*. Prentice-Hall, New Jersey, 1994.

[10] R. L. Garwin, et. al. *Phys. Rev.* **105**, 1415 (1957).

[11] J. Bailey et. al., *Nucl. Phys.* **B150**, 1 (1979).

[12] N. H. Brown et. al., http://arXiv.org/abs/hep-ex/0102017, (Preprint; 2001).

[13] C. Amsler. *Amer. Jour. Phys.* **42**, 1067 (1974).

[14] E. J. Weinberg, D. L. Nordstrom. *Phys. Rev.* **D54**, 21 (1996).

[15] S. Hayakawa. *Cosmic Ray Physics*, (Wiley, New York, 1969), *Monographs and Texts in Physics and Astronomy*, Vol. XXII.

[16] N. T. Tsoulfanidis. *Measurement and Detection of Radiation*. Taylor and Francis, Washington, D.C., 1995.